SUPPORTING INFORMATION

Ligand Exchange on and Allylic C-H Activation by Iron(0) Fragments: π-Complexes, Allyliron Species and Metallacyles

Alicia Casitas,[‡] Helga Krause,[‡] Sigrid Lutz,[‡] Richard Goddard,[‡] Eckhard Bill,[‖] and Alois Fürstner[‡]*

[‡] *Max-Planck-Institut für Kohlenforschung, 45470 Mülheim/Ruhr, Germany*

[‖] *Max-Planck-Institut für Chemische Energiekonversion, 45470 Mülheim/Ruhr, Germany*

Table of Contents

ADDITIONAL CRYSTALLOGRAPHIC INFORMATION

Supporting crystallographic data for this paper can be obtained free of charge from The Cambridge Crystallographic Data Centre via www.ccdc.cam.ac.uk: CCDC 1564812 (**7**), 1564813 (**9**), 1564814 (**10**), 1564815 (**12**), 1564816 (**15**), 1564817 (**23**), 1564818 (**25**), 1564819 (**27**), 1564820 (**32**), 1564821 (**33**), 1564822 (**34**), 1564823 (**35a**), 1564824 (**35b**).

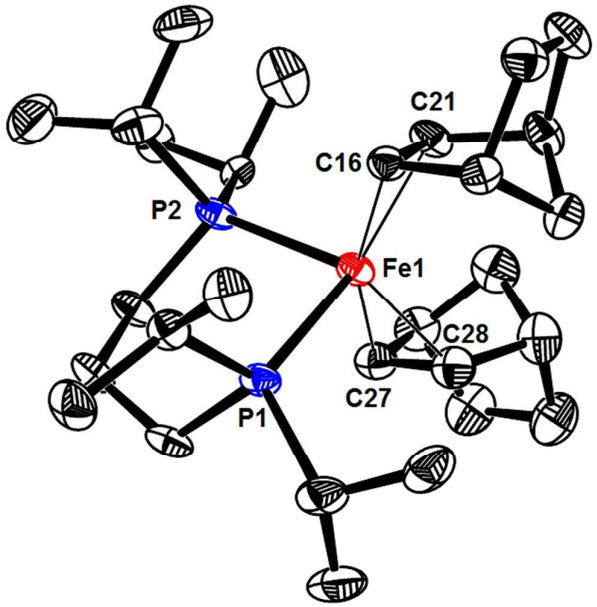

Figure S1. Structure of [(dippp)Fe(norbornene)$_2$] (**10**) in the solid state; disordered solute hexane in the unit cell is not shown for clarity

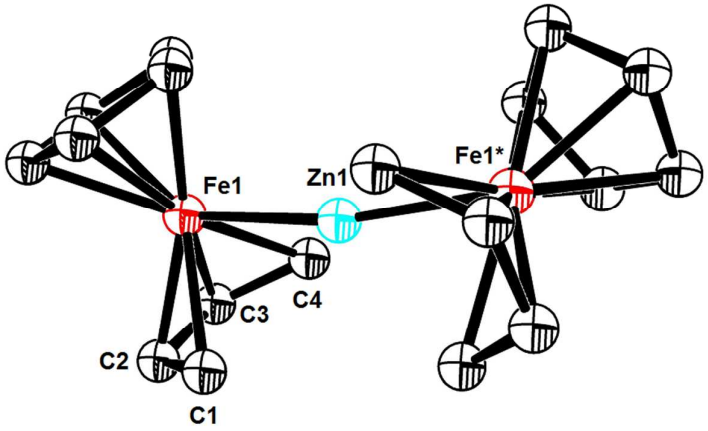

Figure S2. Structure of [CpFe(butadiene)]$_2$Zn (**33**) in the solid state

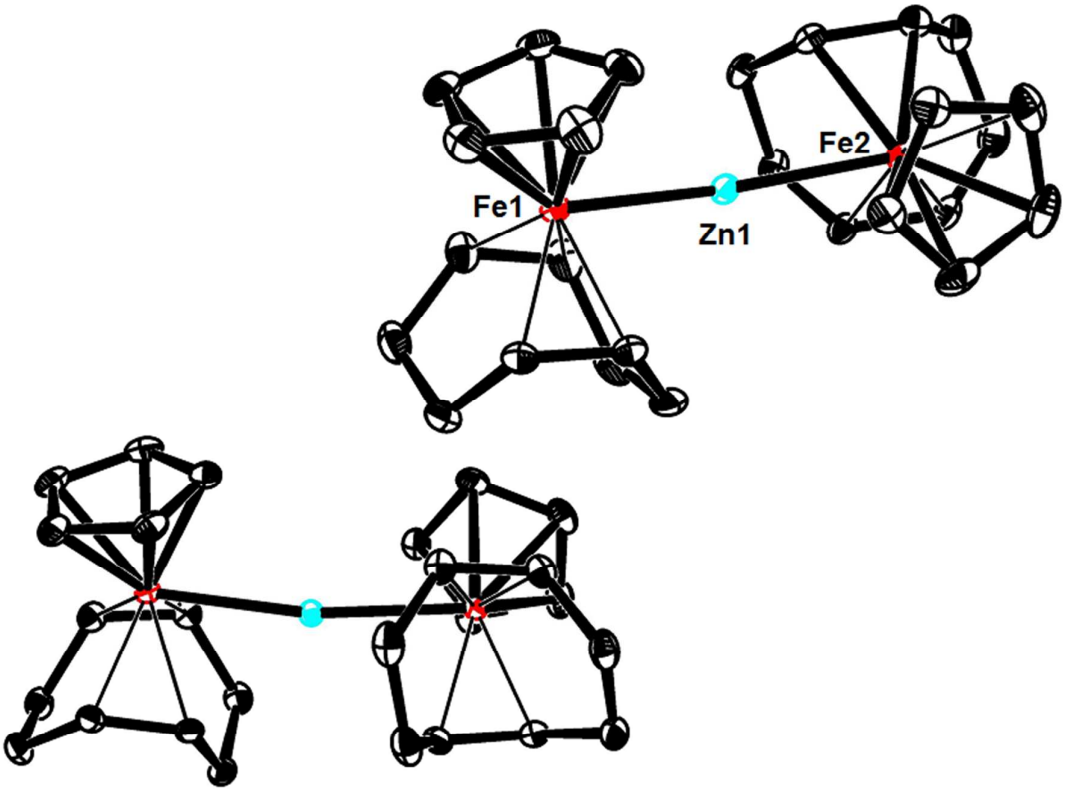

Figure S3. Structure of $[CpFe(cod)]_2Zn$ (**35a**) in the solid state

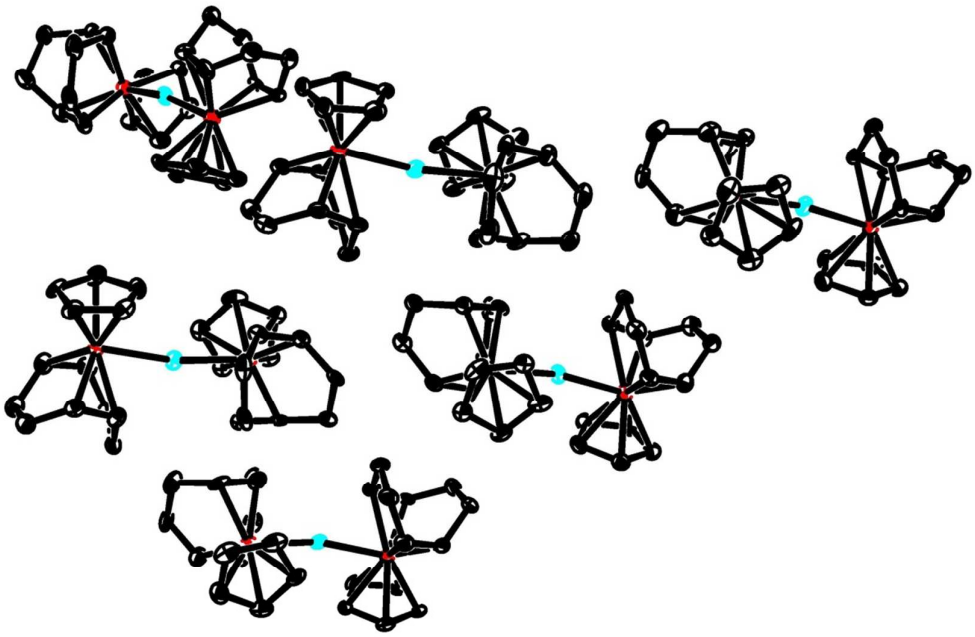

Figure S4. Structure of a second polymorph of $[CpFe(cod)]_2Zn$ (**35b**) in the solid state

^{1}H-NMR (500 MHz, -55°C, THF-d_8) of (dippp)(η^5-C_6H_7Et-*endo*)(H)Fe (20)

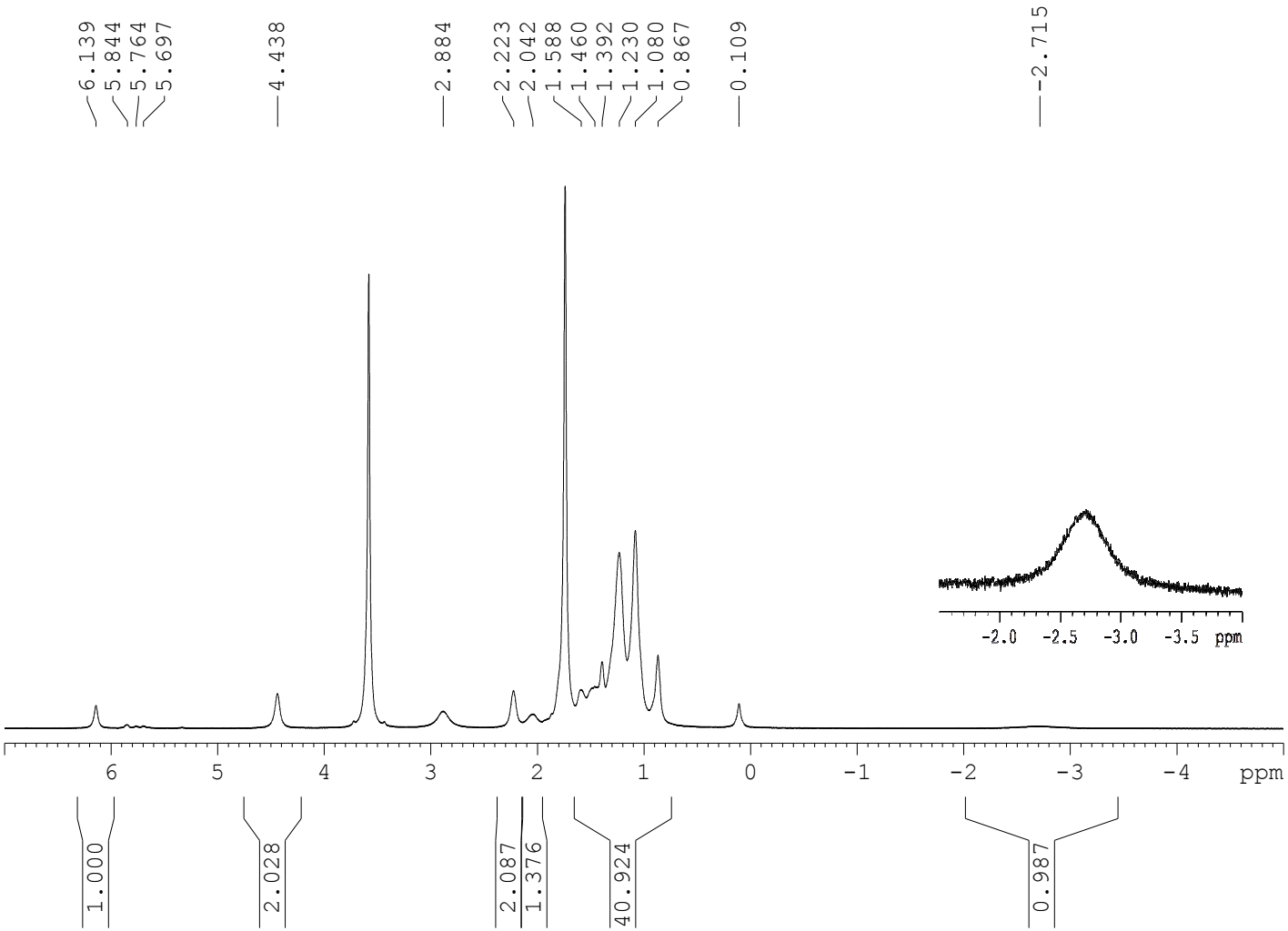

^{13}C-NMR (126 MHz, -55°C, THF-d_8) of (dippp)(η^5-C_6H_7Et-*endo*)(H)Fe (20)

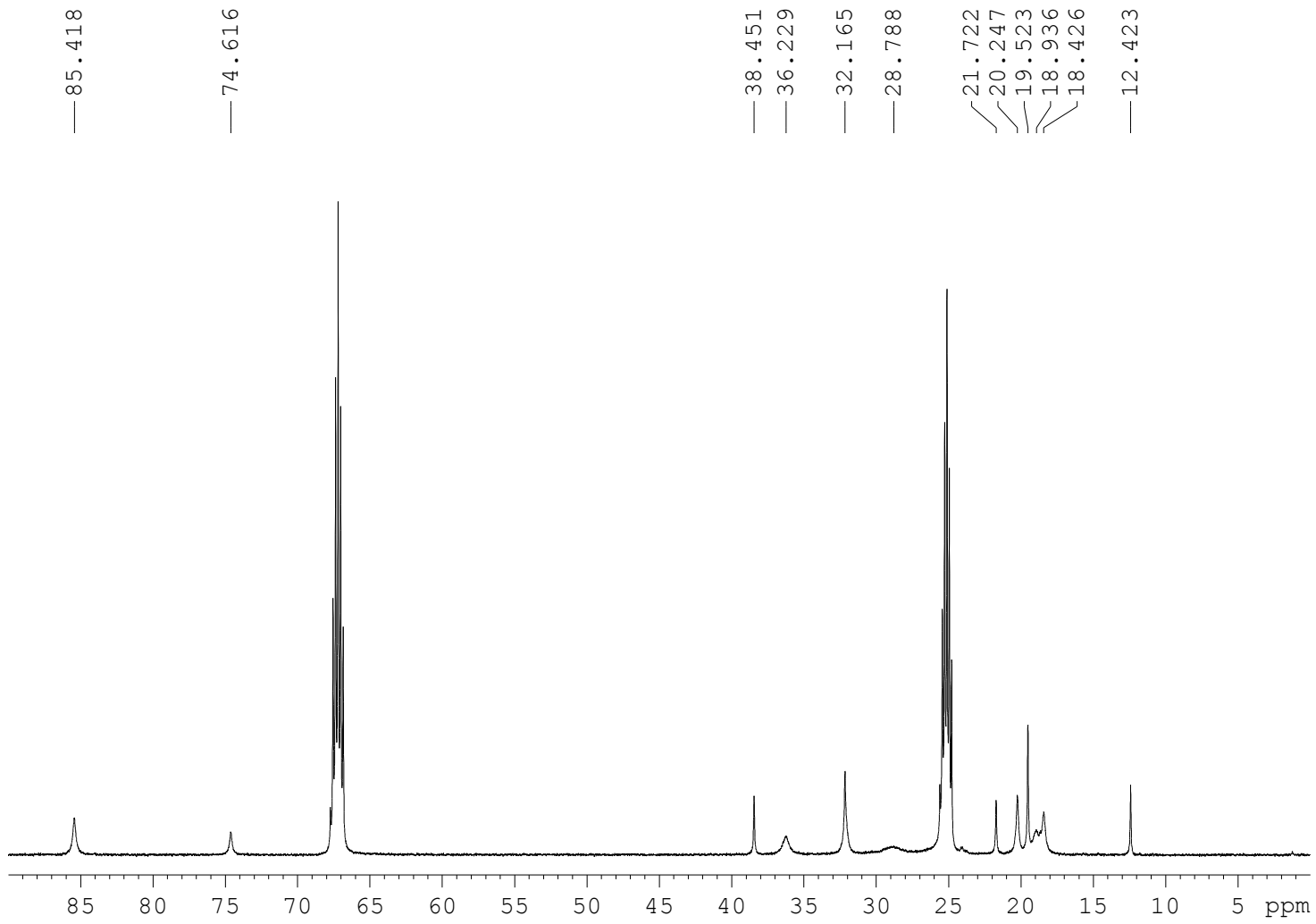

$^{31}P\{^{1}H\}$-NMR (202 MHz, -55°C, THF-d_8) of (dippp)(η^5-C_6H_7Et-*endo*)(H)Fe (20)

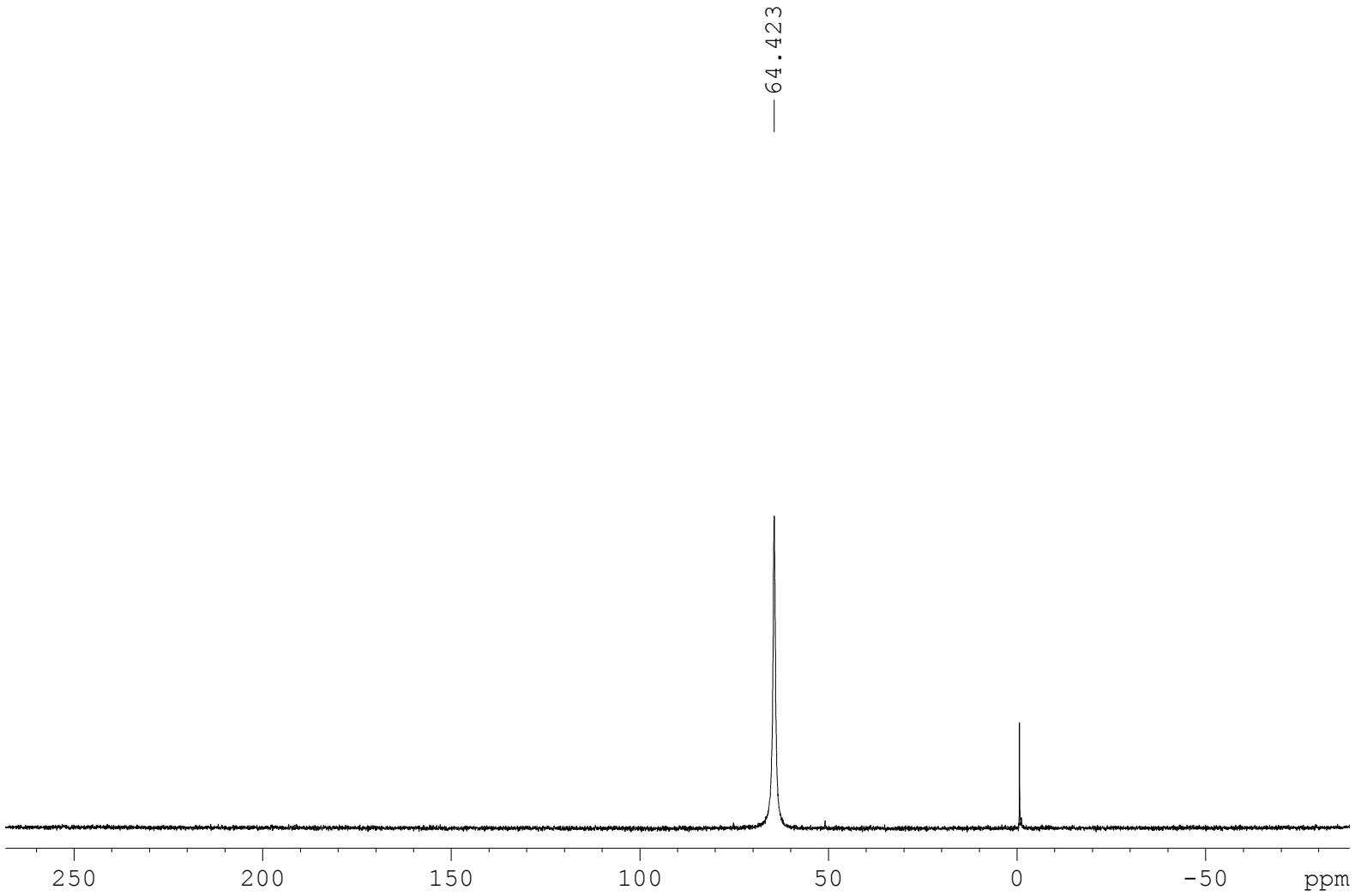

^{1}H-NMR (500 MHz, -55°C, THF-d_8) of (dippe)(η^5-C_5H_5)(Et)Fe (22)

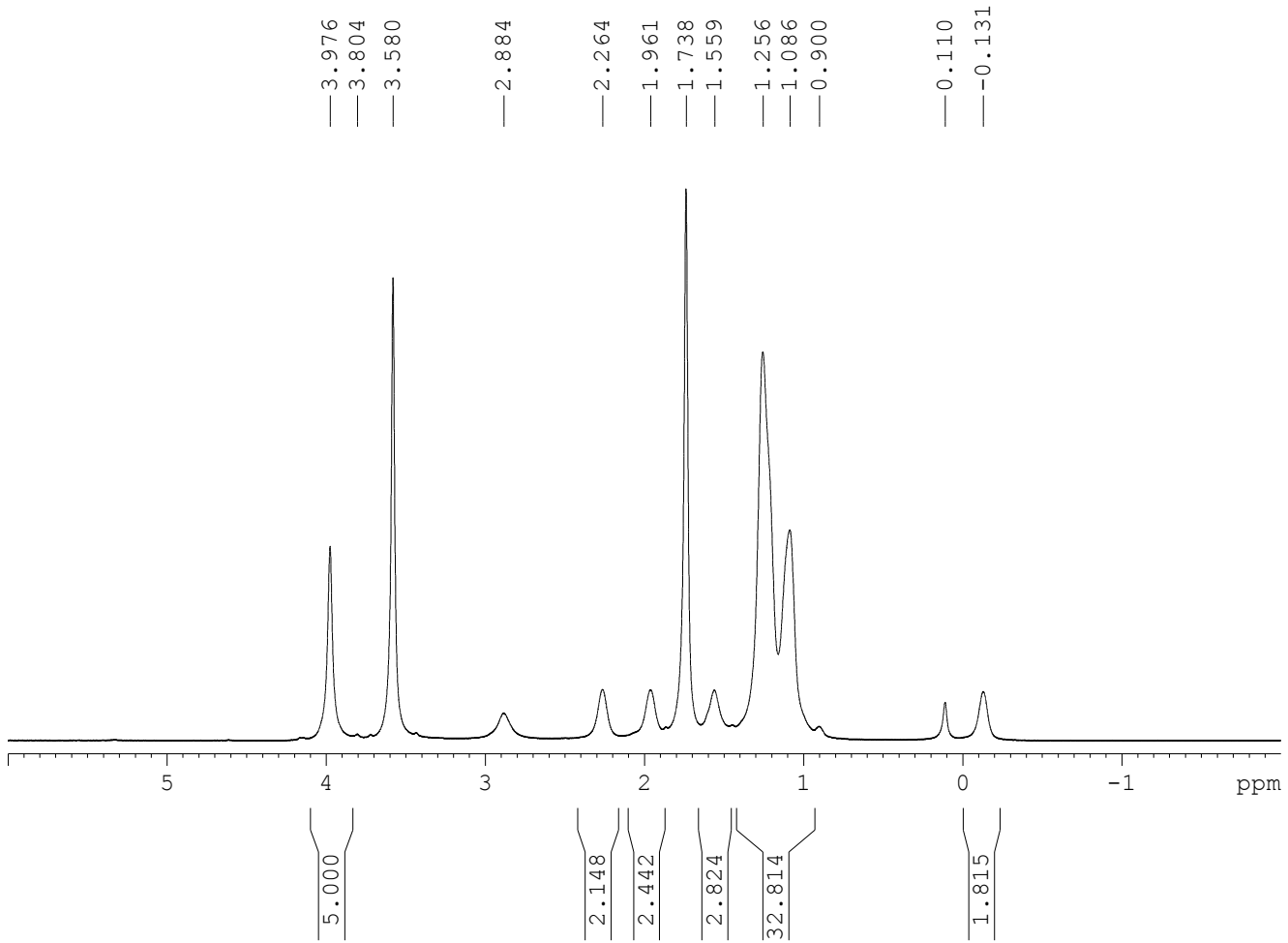

^{13}C-NMR (126 MHz, 25°C, THF-d_8) of (dippe)(η^5-C_5H_5)(Et)Fe (22)

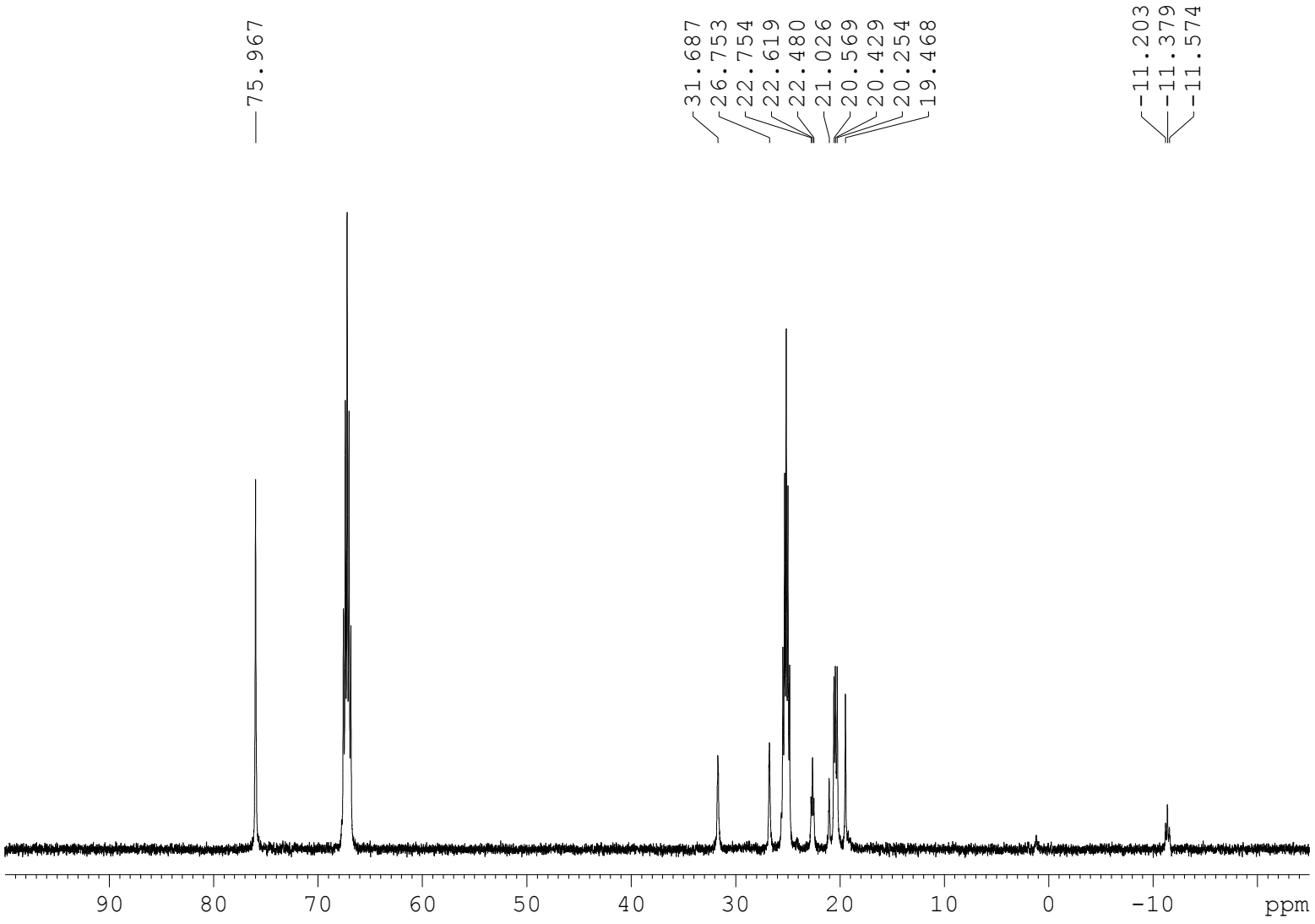

$^{31}P\{^{1}H\}$-NMR (202 MHz, -55°C, THF-d_8) of (dippe)(η^5-C_5H_5)(Et)Fe (22)

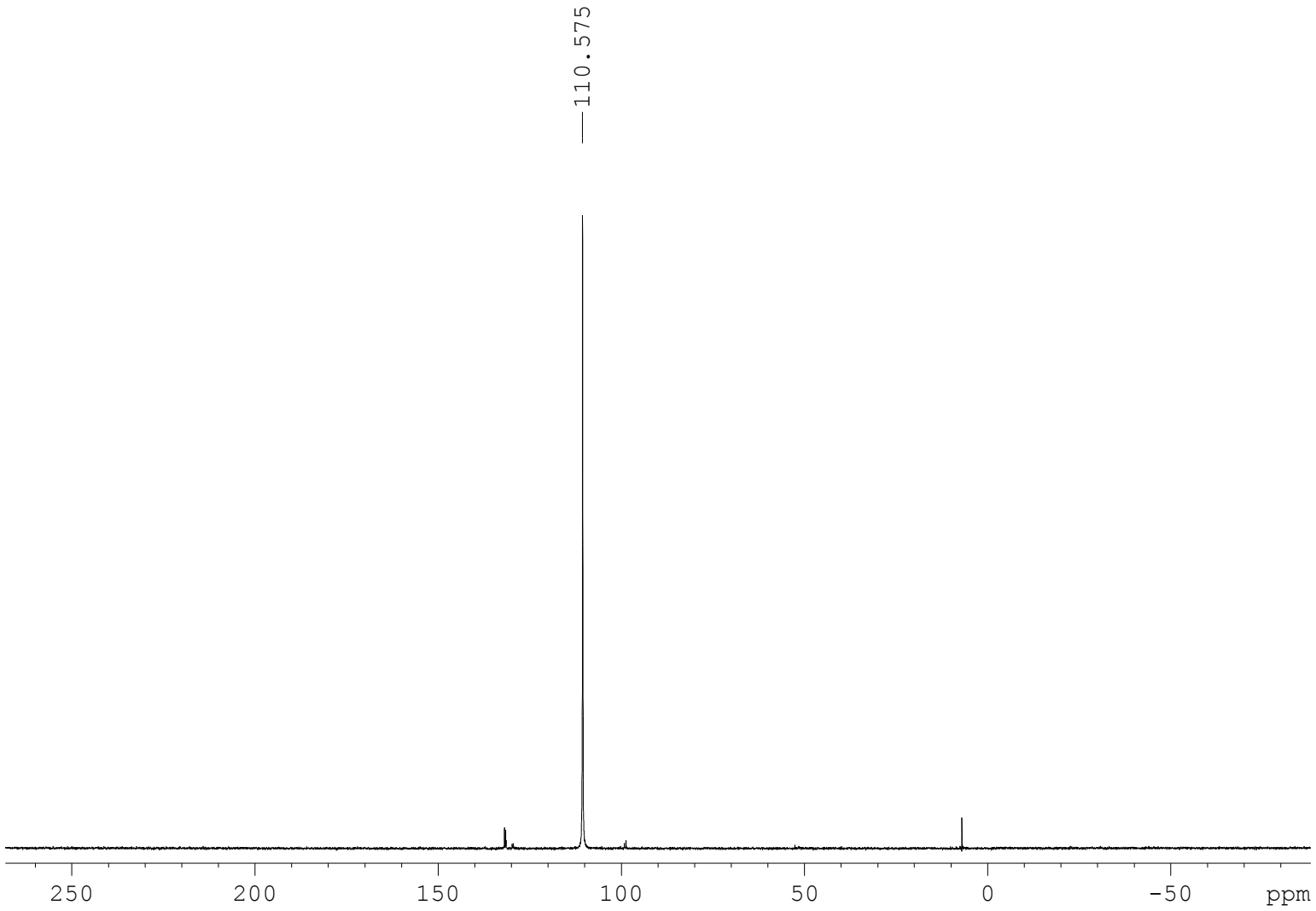

^{1}H-NMR (THF-d_8, -30°C, 500 MHz) of (dippe)(η^5-C_6H_7Et-*endo*)(H)Fe (23)

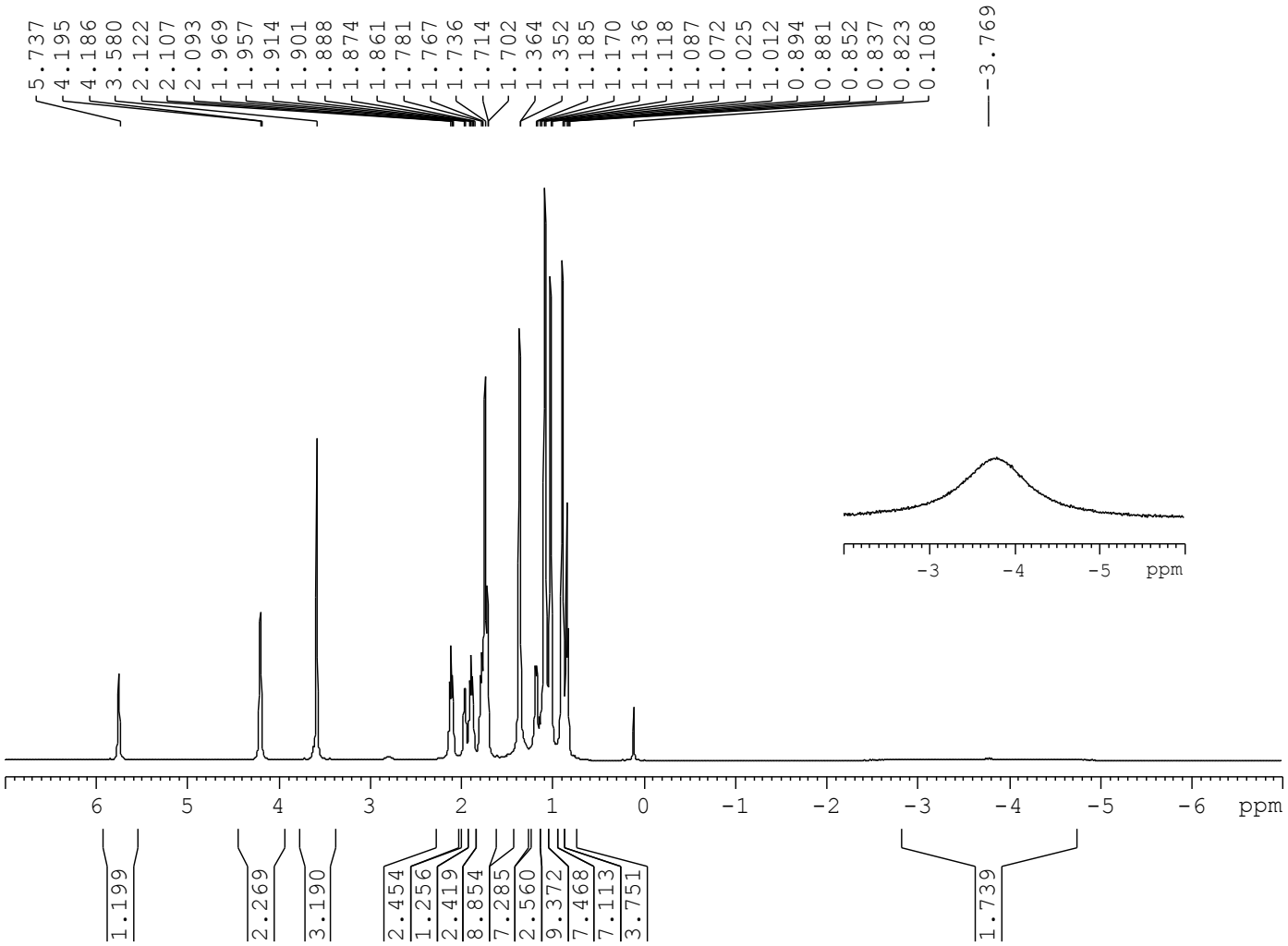

^{13}C-NMR (126 MHz, -30°C, THF-d_8) of (dippe)(η^5-C_6H_7Et-*endo*)(H)Fe (23)

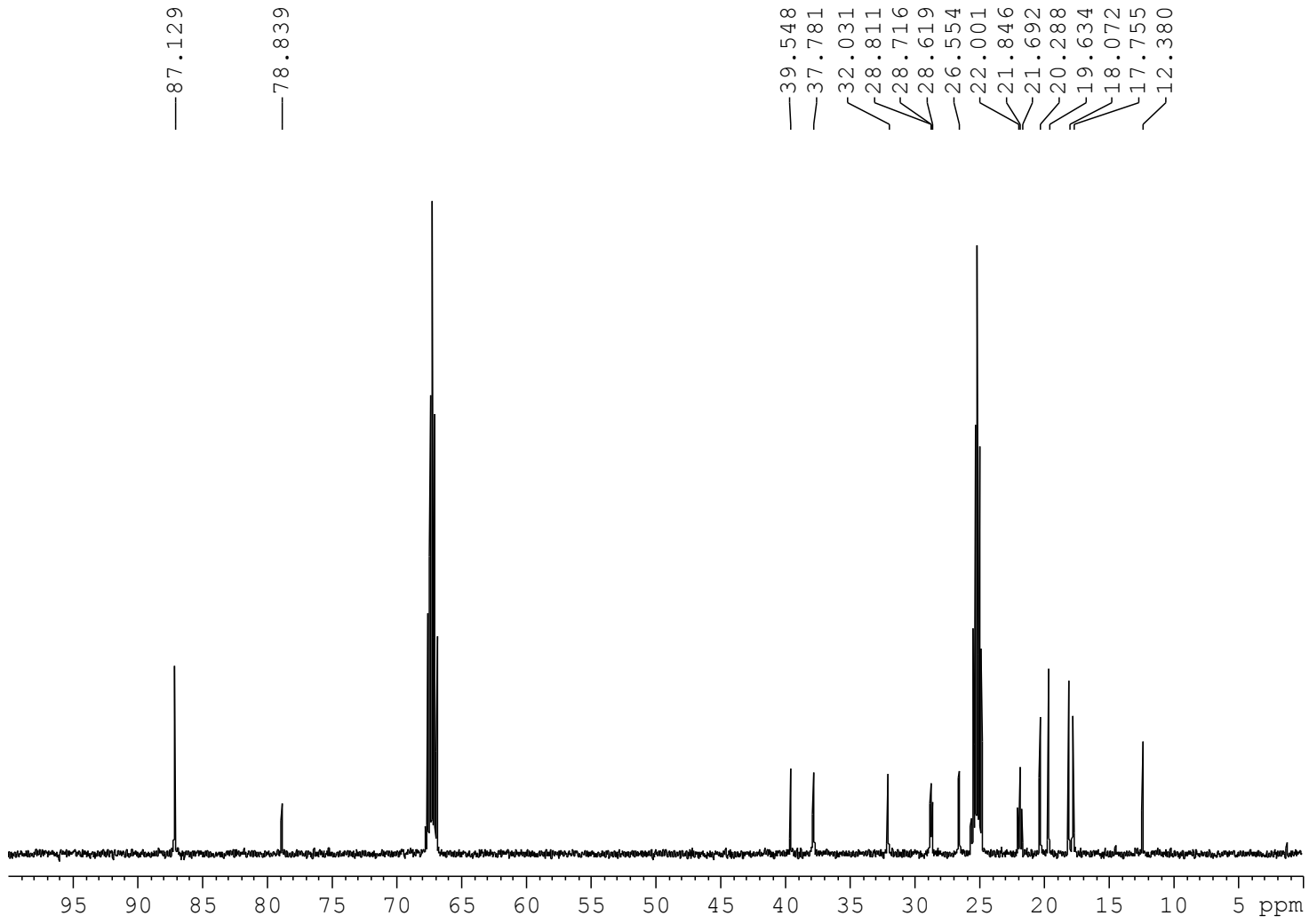

$^{31}P\{^{1}H\}$-NMR (202 MHz, -30°C, THF-d_8) of (dippe)(η^5-C_6H_7Et-*endo*)(H)Fe (23)

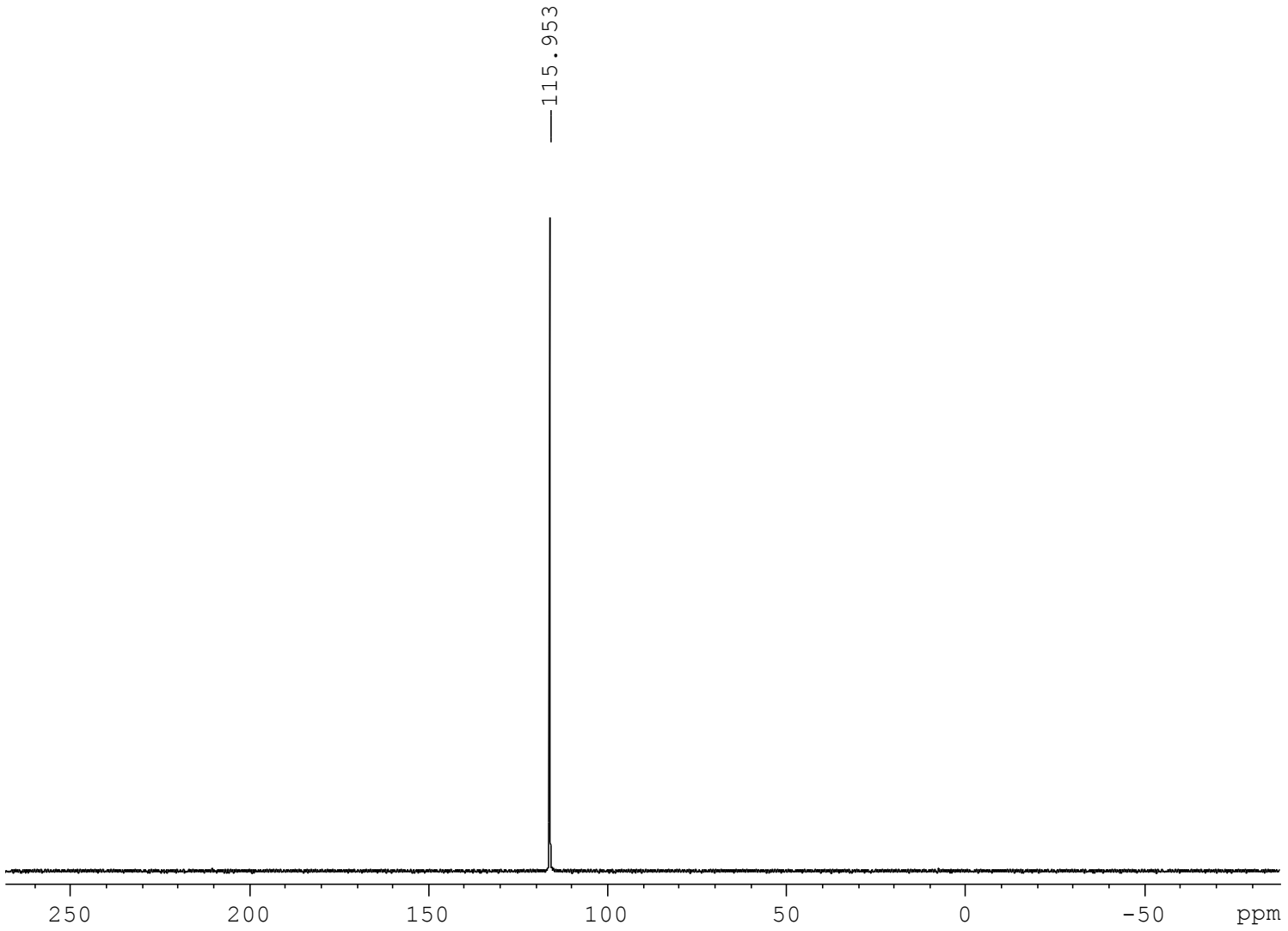

^{1}H-NMR (400 MHz, 193K, THF-d_8) of $[CpFe(ethylene)_2]_2Zn$ (32)

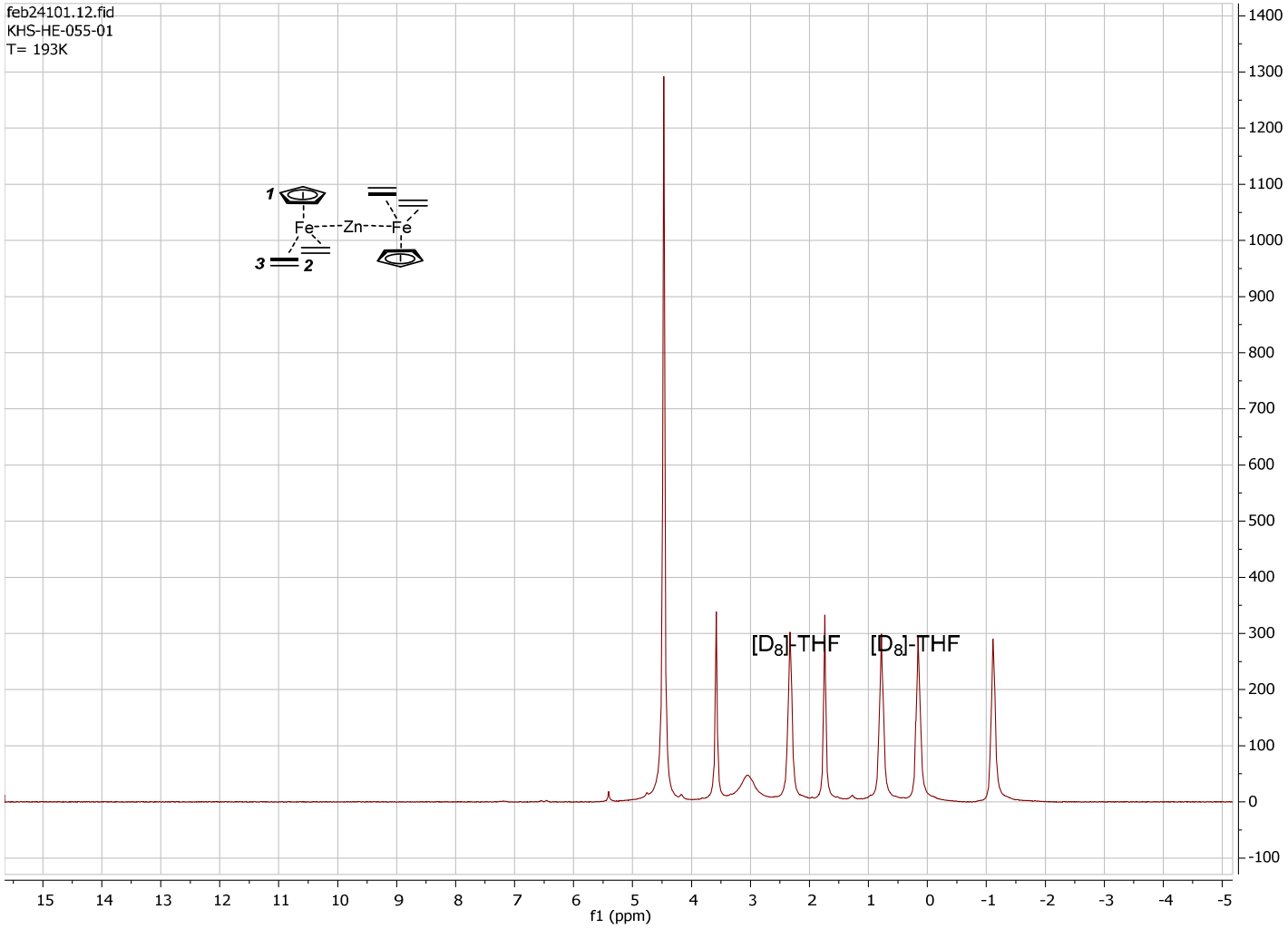

^{13}C-NMR (400 MHz, 193K, THF-d_8) of $[CpFe(ethylene)_2]_2Zn$ (32)

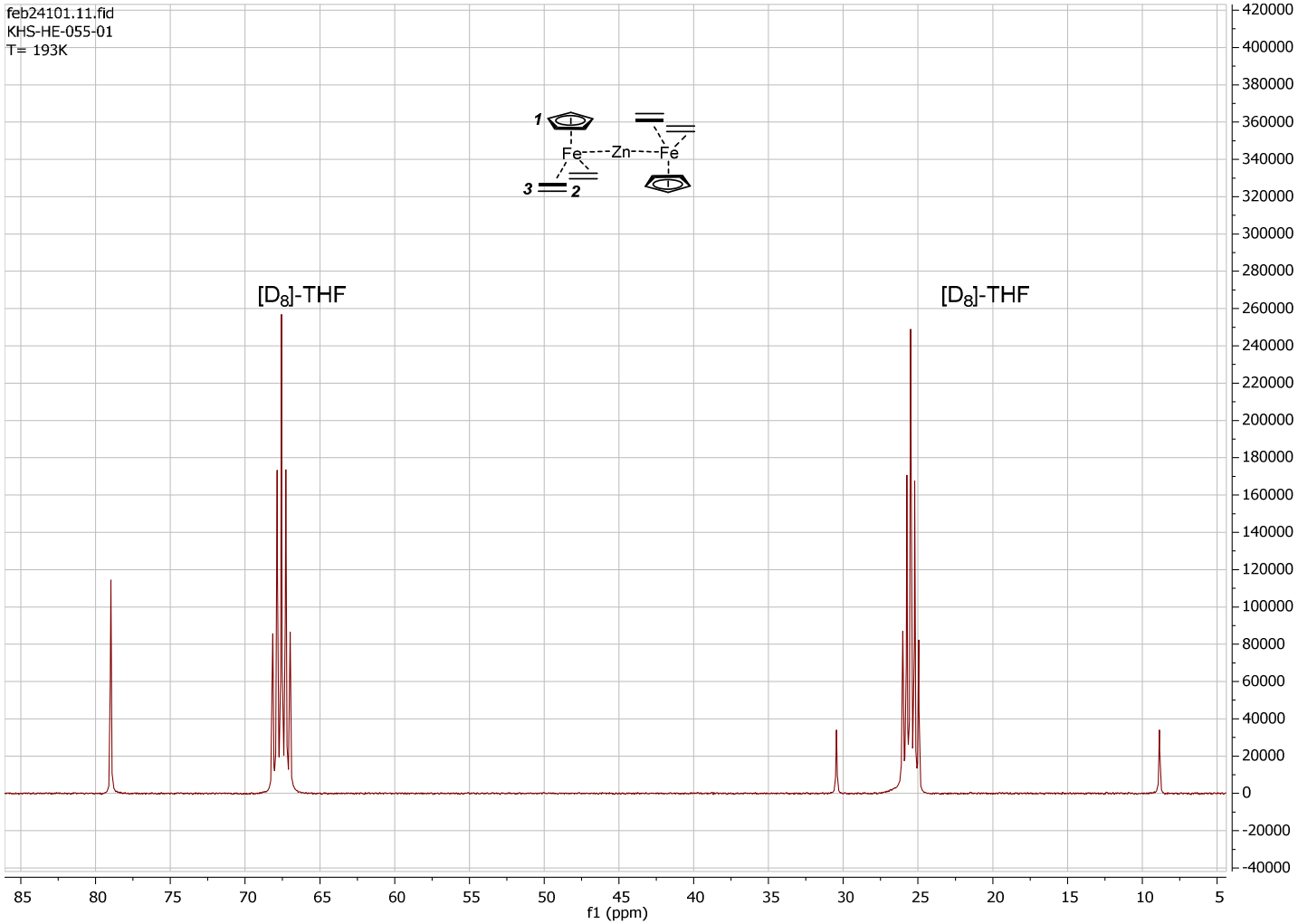

^{1}H-NMR (400 MHz, THF-d_8) of [CpFe(butadiene)]$_2$Zn (33)

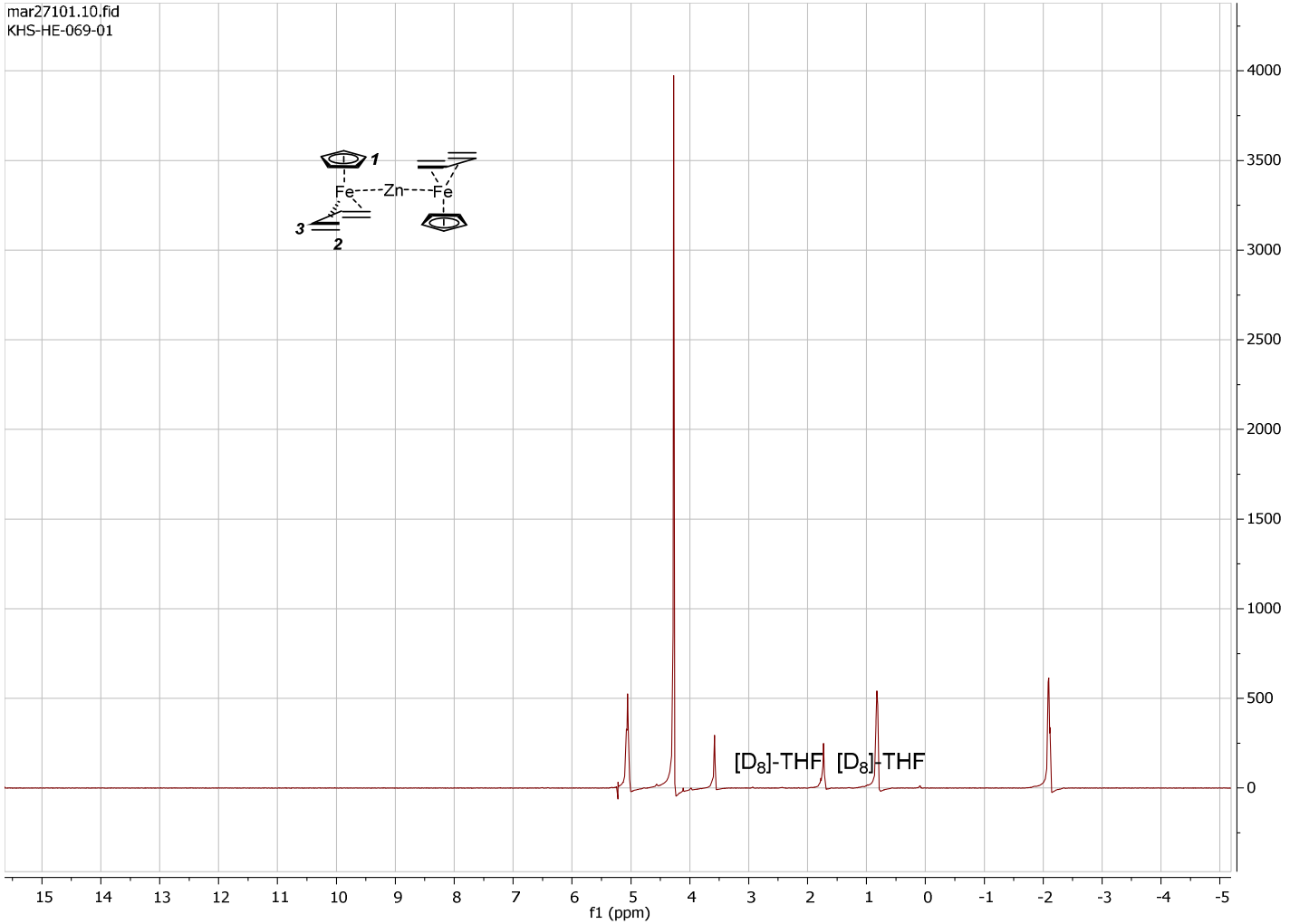

^{13}C-NMR (400 MHz, THF-d_8) of [CpFe(butadiene)]$_2$Zn (33)

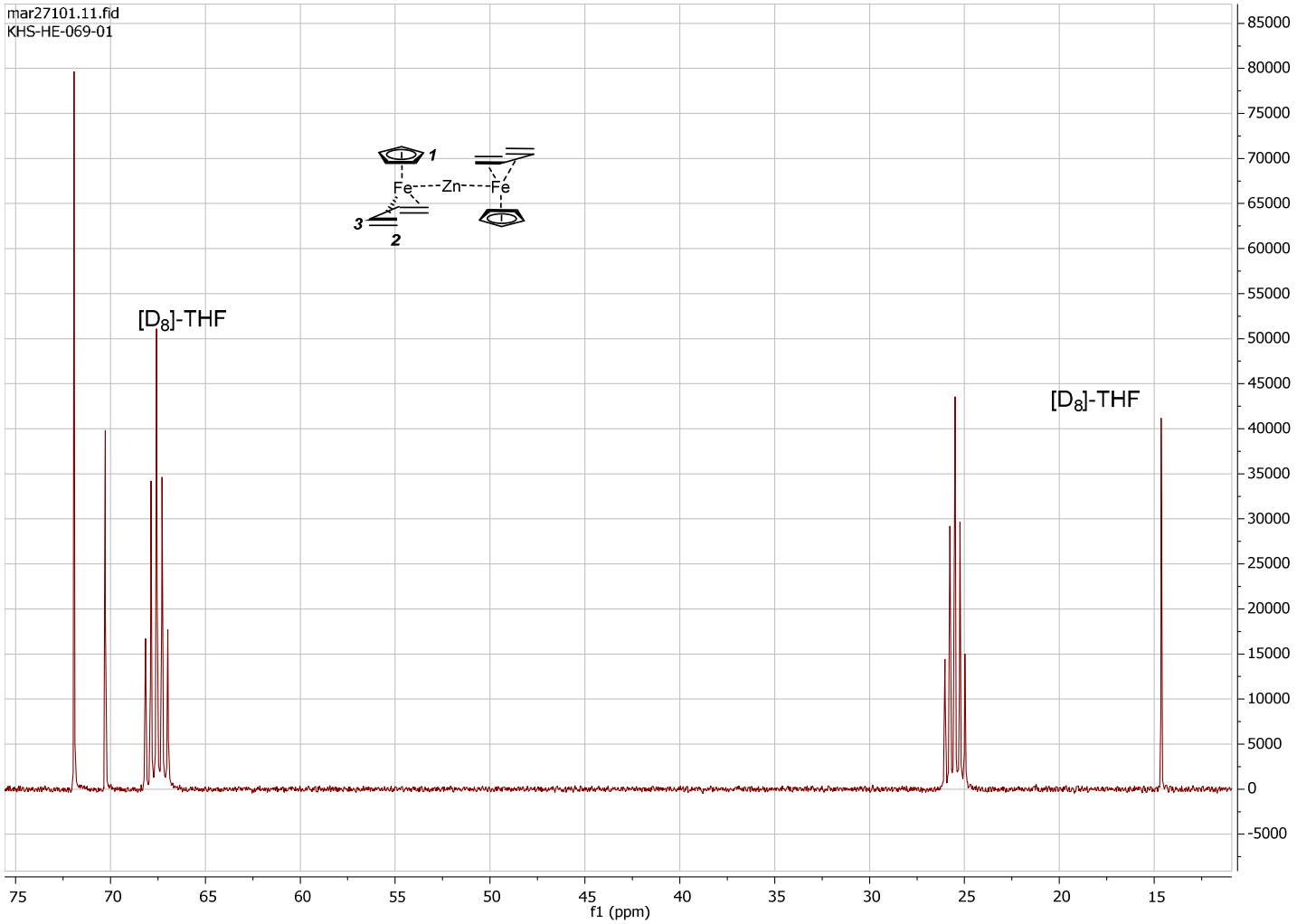

^{13}C-NMR (400 MHz, THF-d_8) of [CpFe(butadiene)]Li (34)

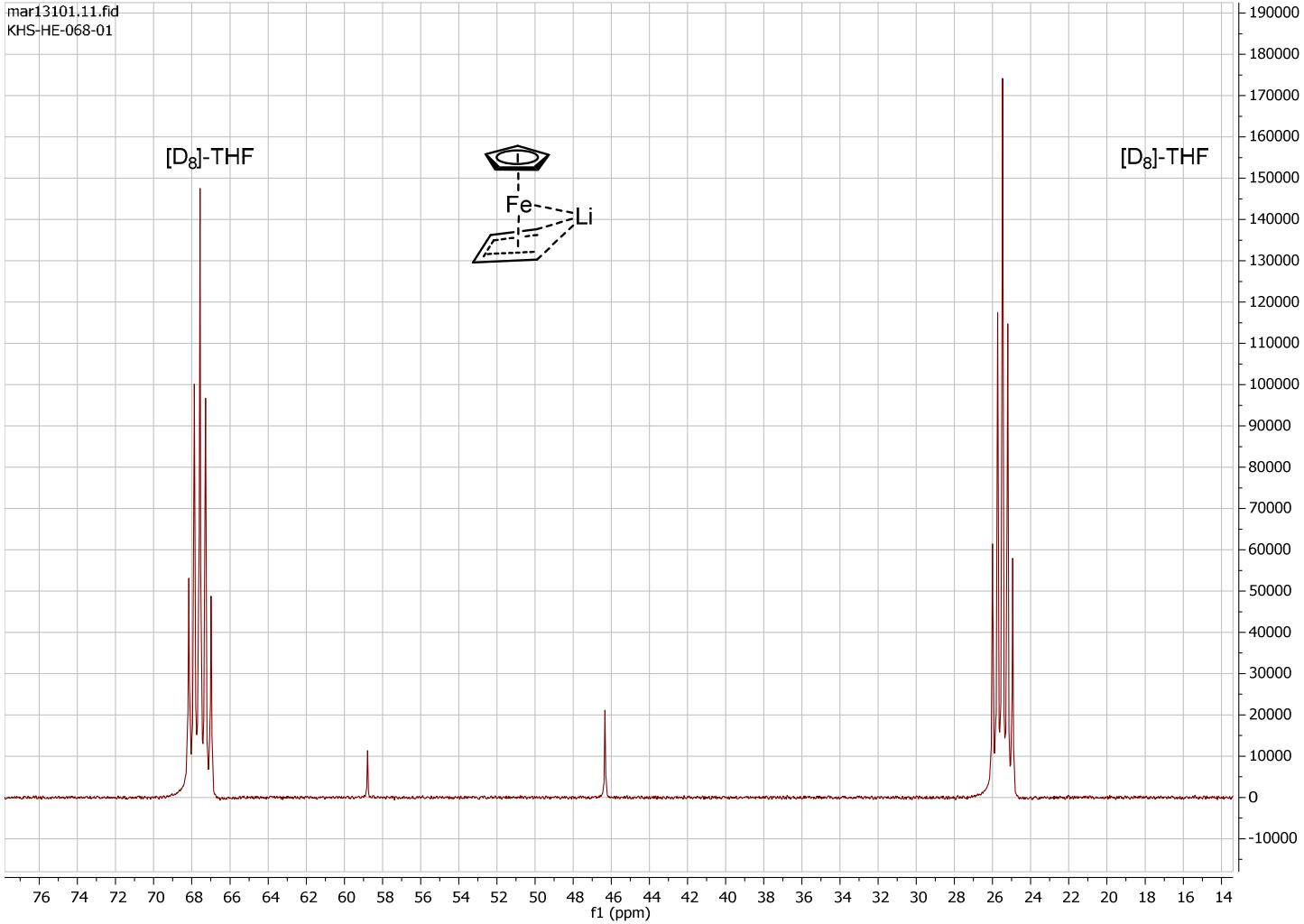

^{1}H-NMR (400 MHz, THF-d_8) of $[CpFe(cod)]_2Zn$ (35)

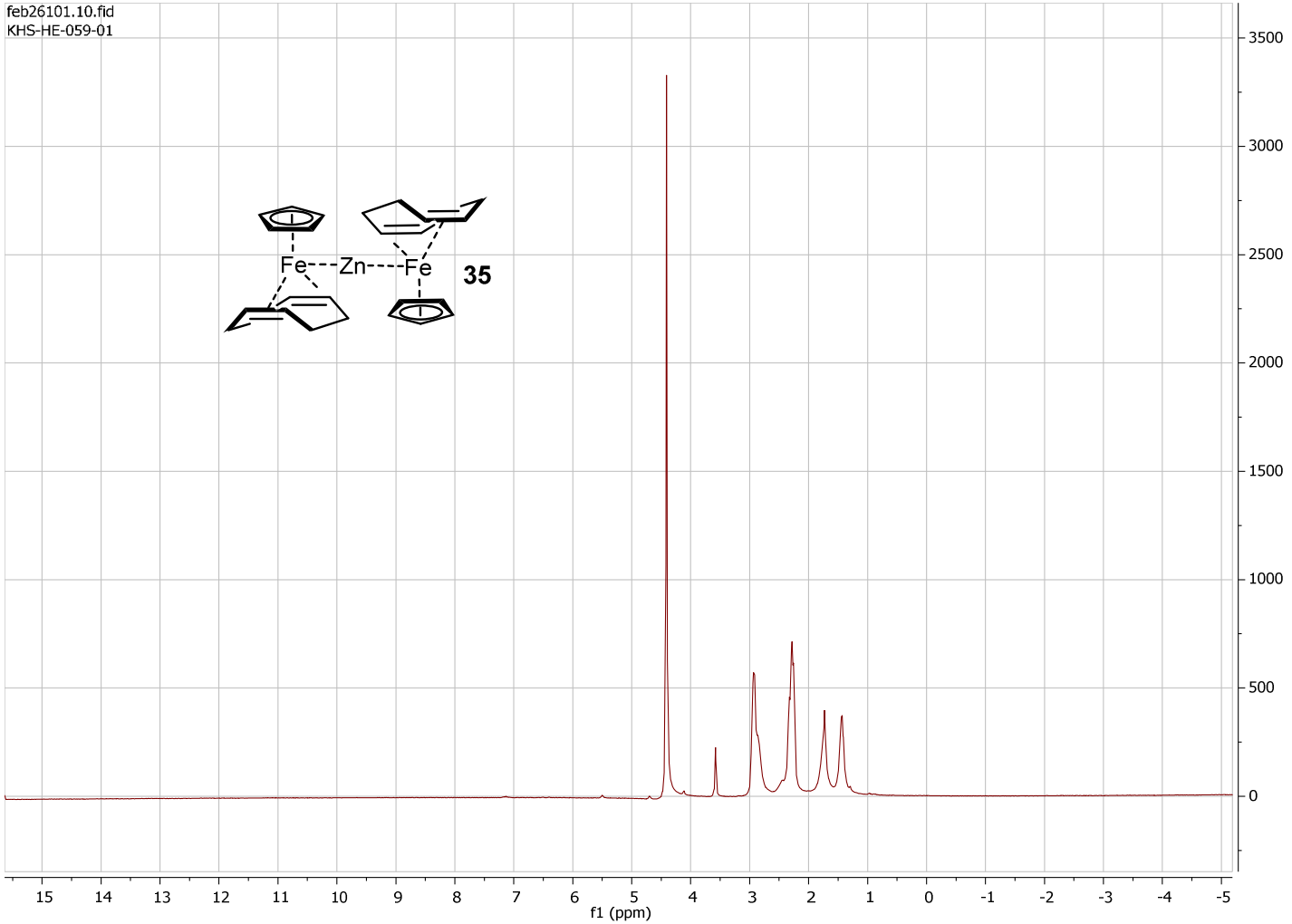

^{13}C-NMR (400 MHz, THF-d_8) of $[CpFe(cod)]_2Zn$ (35)

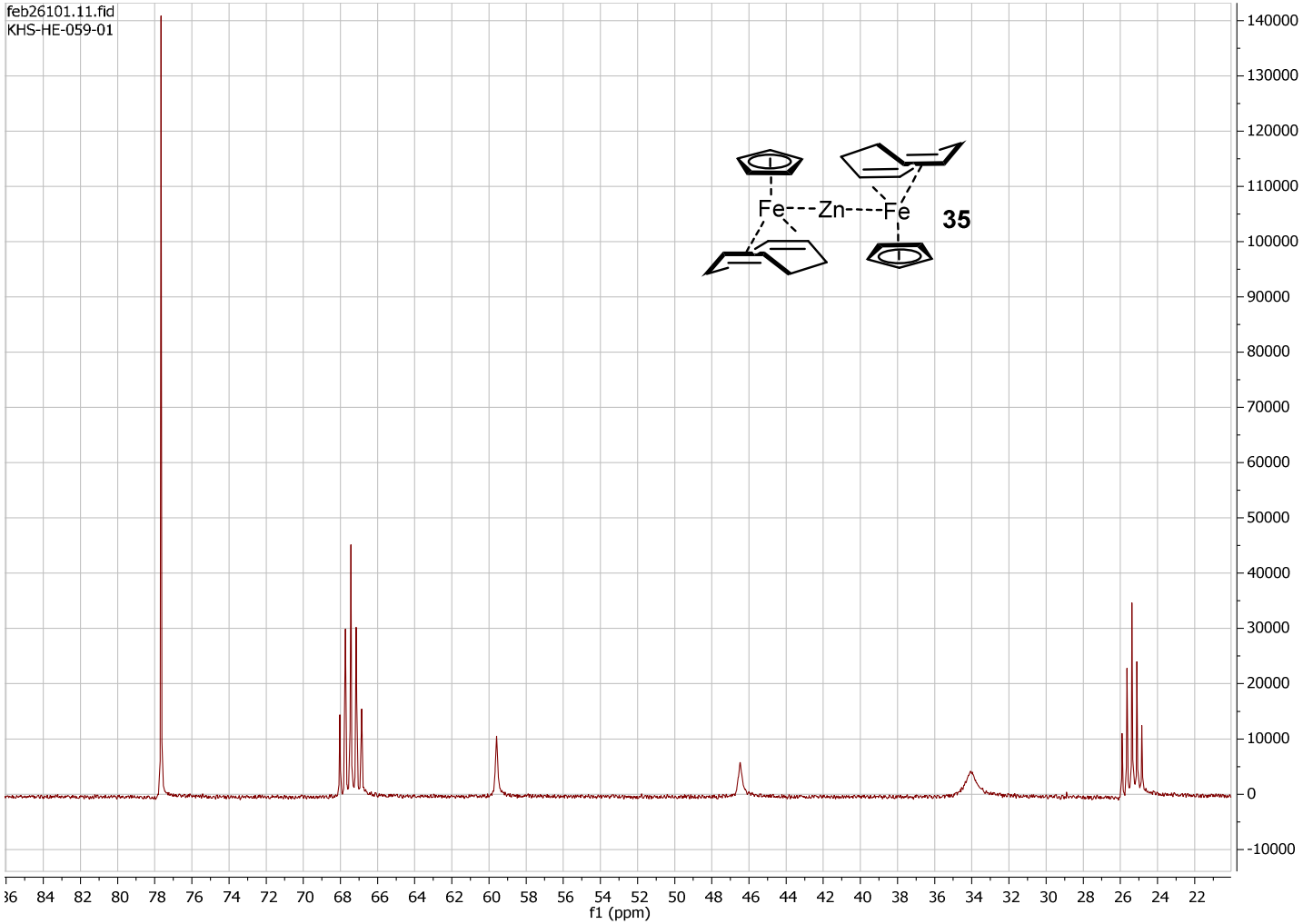

Comparison of the ^{13}C NMR Spectra of Heterometallic π-Complexes Comprising [CpFe] Fragments

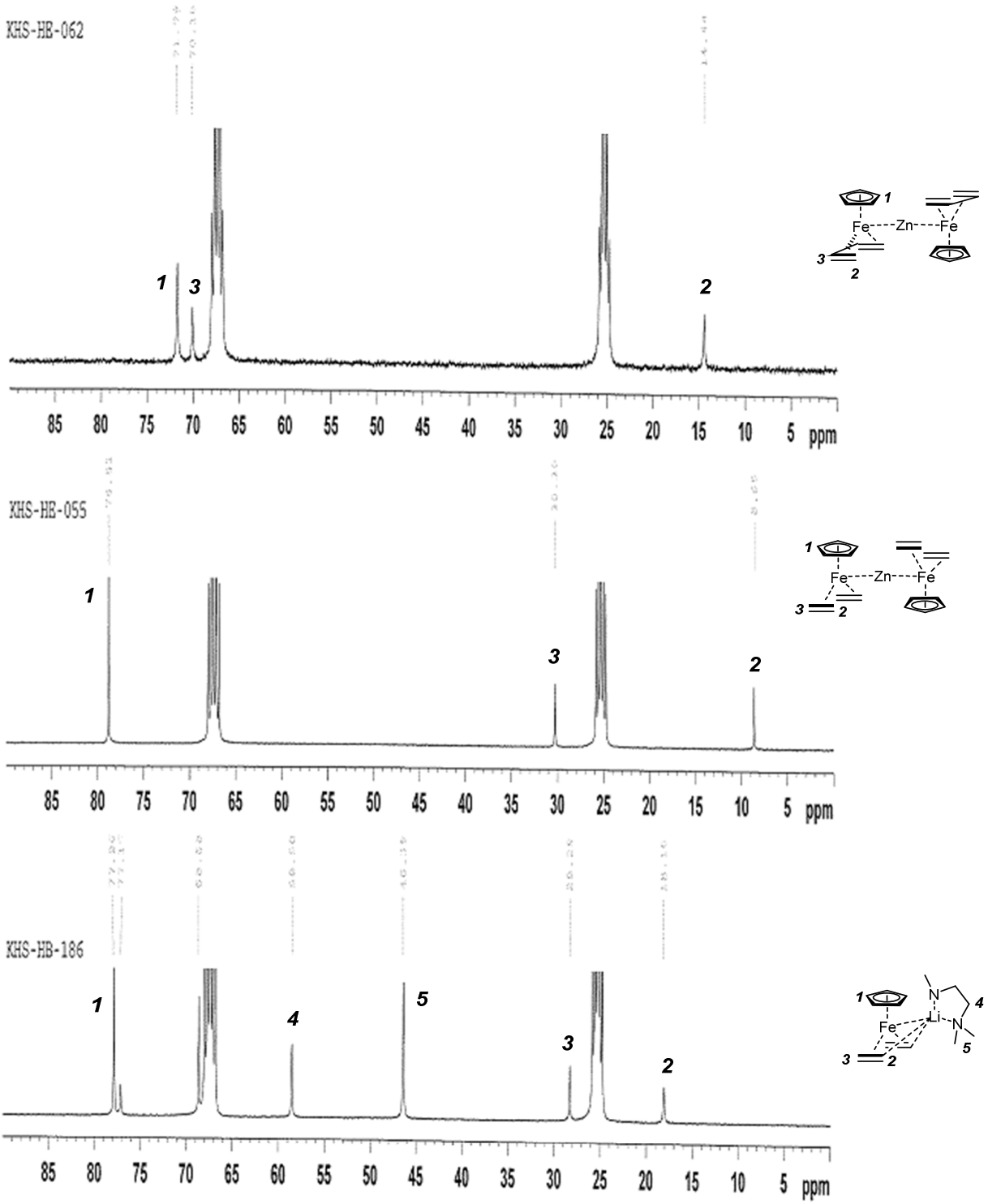

MÖSSBAUER SPECTRA OF SELECTED COMPOUNDS

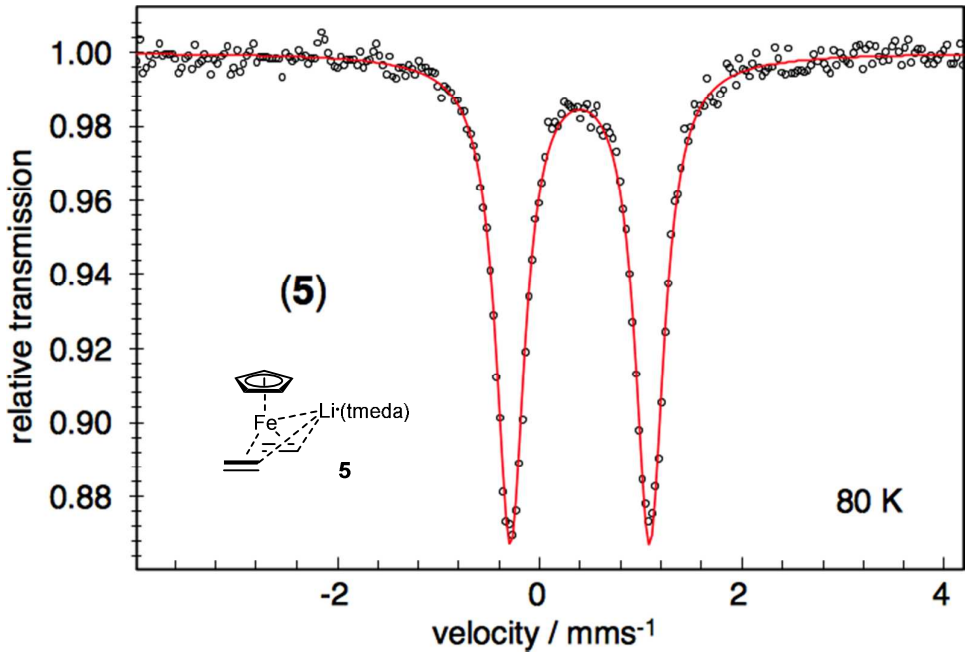

Figure S5. Zero-field Mössbauer spectrum of complex **5** recorded at 80 K (dots). The red line represents a fit with a Lorentzian quadrupole doublet.

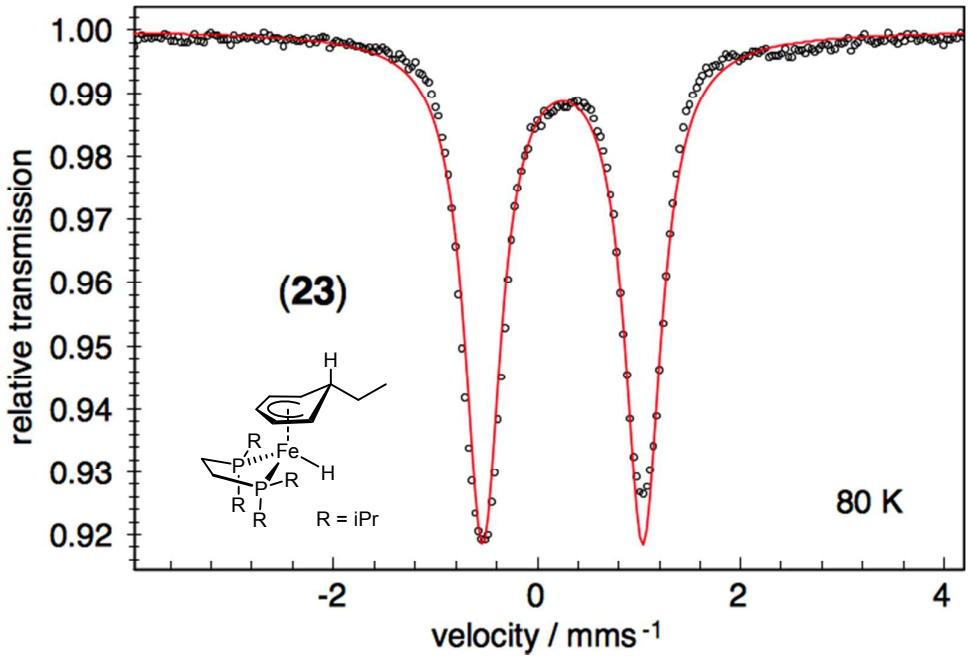

Figure S6. Zero-field Mössbauer spectrum of complex **23** recorded at 80 K (dots). The red line represents a fit with a Lorentzian quadrupole doublet.

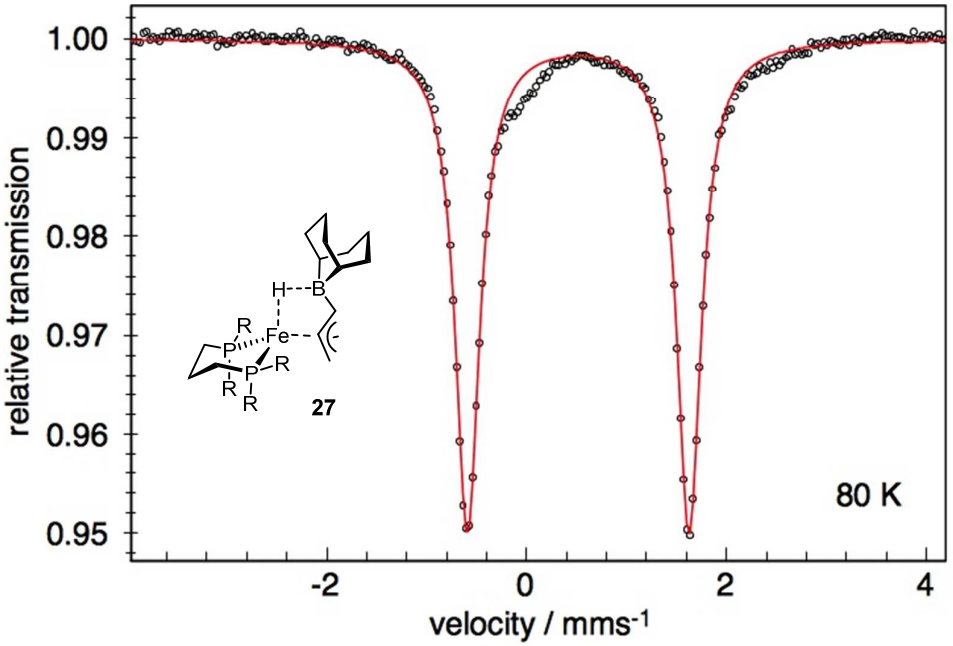

Figure S7. Zero-field Mössbauer spectrum of complex **27** recorded at 80 K (dots). The red line represents a fit with a Lorentzian quadrupole doublet (see Table 1, Experimental Section). The deviations at ca. 0 and 2 mm/s indicates a 12% impurity with an unknown Fe(II) species.

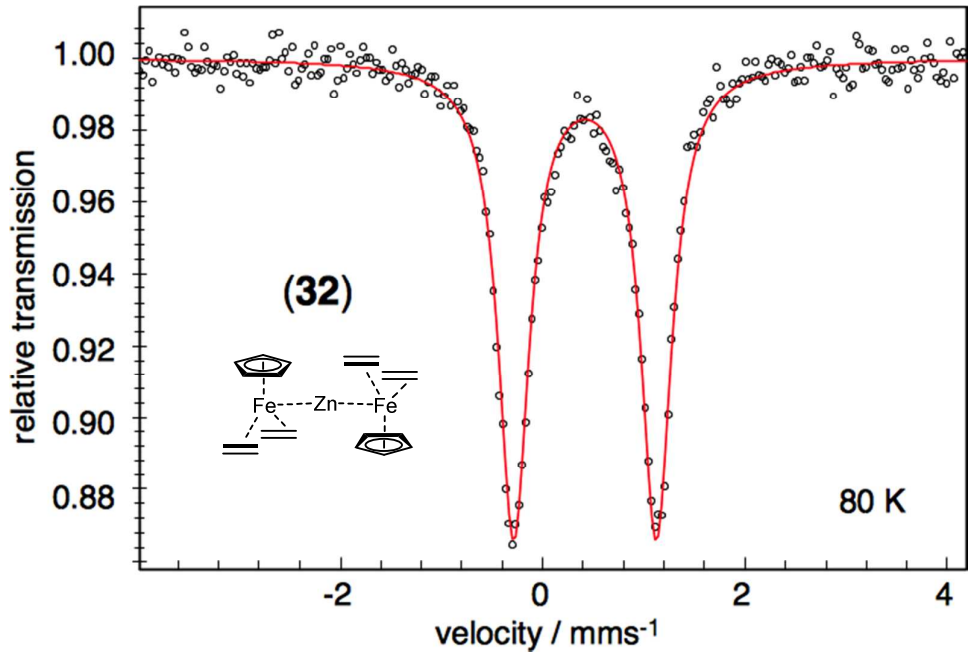

Figure S8. Zero-field Mössbauer spectrum of complex **32** recorded at 80 K (dots). The red line represents a fit with a Lorentzian quadrupole doublet.

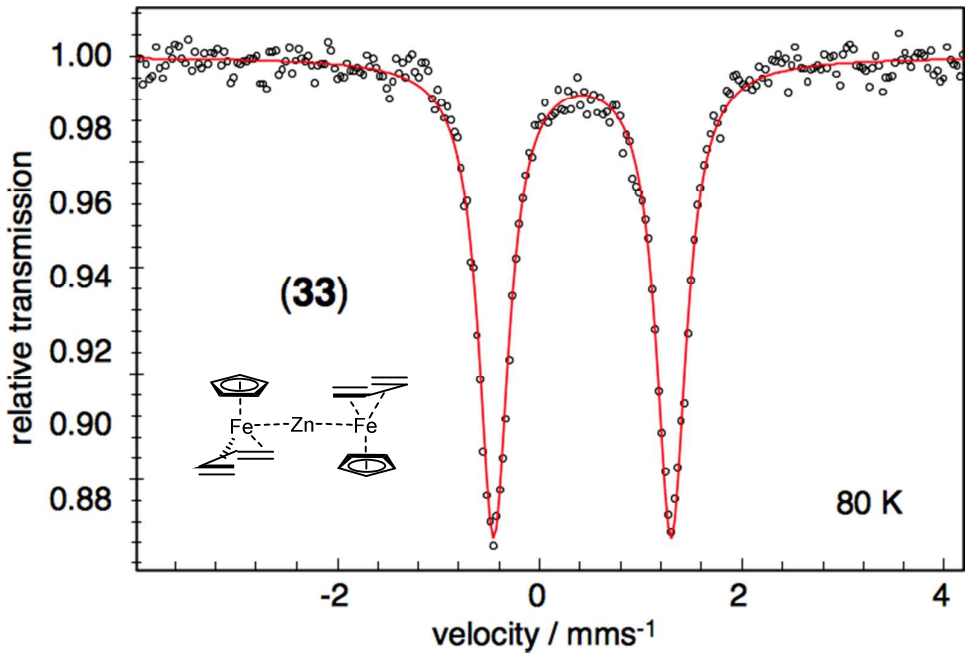

Figure S9. Zero-field Mössbauer spectrum of complex **33** recorded at 80 K (dots). The red line represents a fit with a Lorentzian quadrupole doublet.

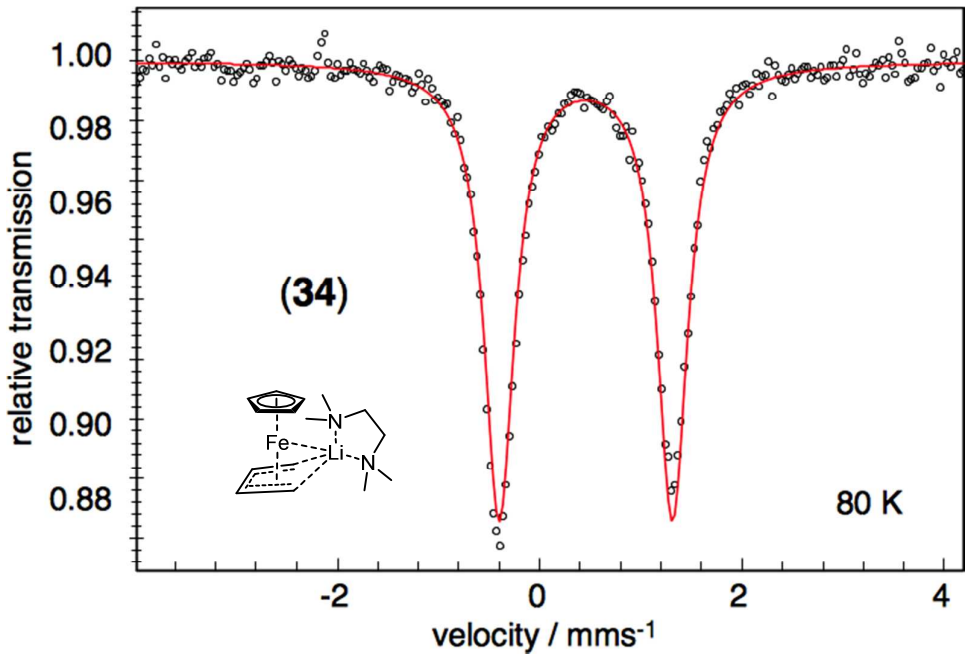

Figure S10. Zero-field Mössbauer spectrum of complex **34** recorded at 80 K (dots). The red line represents a fit with a Lorentzian quadrupole doublet.